

REVIEW ARTICLE

# Engineering bio-inks for 3D bioprinting cell mechanical microenvironment

Yanshen Yang<sup>1,2</sup>, Yuanbo Jia<sup>1,2</sup>, Qingzhen Yang<sup>1,2</sup>, Feng Xu<sup>1,2\*</sup>

<sup>1</sup>The Key Laboratory of Biomedical Information Engineering of Ministry of Education, School of Life Science and Technology, Xi'an Jiaotong University, Xi'an, Shaanxi, 710049, P.R. China

<sup>2</sup>Bioinspired Engineering and Biomechanics Center (BEBC), Xi'an Jiaotong University, Xi'an, Shaanxi, 710049, P.R. China

(This article belongs to the *Special Issue: Composite/Multi-component Biomaterial Inks and Bioinks*)

## Abstract

Three-dimensional (3D) bioprinting has become a promising approach to constructing functional biomimetic tissues for tissue engineering and regenerative medicine. In 3D bioprinting, bio-inks are essential for the construction of cell microenvironment, thus affecting the biomimetic design and regenerative efficiency. Mechanical properties are one of the essential aspects of microenvironment, which can be characterized by matrix stiffness, viscoelasticity, topography, and dynamic mechanical stimulation. With the recent advances in functional biomaterials, various engineered bio-inks have realized the possibility of engineering cell mechanical microenvironment *in vivo*. In this review, we summarize the critical mechanical cues of cell microenvironments, review the engineered bio-inks while focusing on the selection principles for constructing cell mechanical microenvironments, and discuss the challenges facing this field and the possible solutions for them.

\*Corresponding author:  
Feng Xu (fengxu@mail.xjtu.edu.cn)

**Citation:** Yang Y, Jia Y, Yang Q, *et al.*, 2023, Engineering bio-inks for 3D bioprinting cell mechanical microenvironment. *Int J Bioprint*, 9(1): 632.  
<https://doi.org/10.18063/ijb.v9i1.632>

**Received:** June 21, 2022  
**Accepted:** August 29, 2022  
**Published Online:** October 29, 2022

**Copyright:** © 2022 Author(s). This is an Open Access article distributed under the terms of the Creative Commons Attribution License, permitting distribution and reproduction in any medium, provided the original work is properly cited.

**Publisher's Note:** Whioce Publishing remains neutral with regard to jurisdictional claims in published maps and institutional affiliations.

**Keywords:** Biofabrication; Mechanical microenvironment; Bioprinting; Bio-inks

## 1. Introduction

In tissue engineering, using engineered biomaterials that are integrated with seed cells is an important strategy to construct functional tissues *in vitro* for implantation<sup>[1]</sup>. However, the existing tissue engineering methods are unable to attain the expected therapeutic effect of ideal regenerative medicine. The reason for this is the inability to precisely regulate cell behavior to achieve regenerative needs<sup>[2]</sup>. All processes from *in vitro* functional tissue construction to post-implantation integration with the body involve complex interactions between cells and biomaterials or extracellular matrix (ECM)<sup>[3]</sup>. A deep understanding of how cells sense and interact with the surrounding microenvironment is essential for tissue engineering.

The state of cells in living tissues is not independent, as it is affected by the surrounding environment and responds accordingly. The environment at the cellular scale is considered to be the cell's microenvironment. Cell microenvironment is a superposition of many components, including neighboring cells, ECM, soluble factors, and physical cues, which can be further classified as chemical and physical microenvironments<sup>[4]</sup>. For example, the physiological state of skeletal muscle is influenced by the concentration of

extracellular calcium ions and the activation of electrical signals from the nervous system<sup>[5]</sup>. Its physiological state is also maintained by mechanical stress<sup>[6]</sup>. The neuromuscular junction, which allows cell-to-cell interaction, triggers action potentials in muscle cells; the concentration of extracellular calcium ions, which determines the excitability of muscle cells, is the chemical microenvironment, whereas the tension of tendon stretching muscle cells is the mechanical microenvironment. The activity of cells is highly dependent on the microenvironment; hence, cells are prompted to make adaptive changes in face of fluctuations in the microenvironment. This may lead to a series of physiological changes or even pathological system imbalances<sup>[7]</sup>.

The mechanical microenvironment has not yet been fully explored, unlike the chemical microenvironment, which has been extensively investigated. In the past two decades, a growing line of evidence has shown that mechanical microenvironment plays a crucial role in regulating cell behaviors<sup>[8]</sup>. Matrix stiffness, viscoelasticity, topography, and dynamic mechanical stimulation are all included in the cell mechanical microenvironment; synergistically, they determine the cell fate<sup>[4]</sup>. For instance, multipotent stromal cells can differentiate into bone, cartilage, or skeletal muscle tissue, depending on different matrix stiffnesses<sup>[9]</sup>. Cells probe the mechanical microenvironment in various ways, and even if they are not adherent, cells in suspension rely on mechanical signals. Platelets control the coagulation process by sensing the stiffness of fibrin networks and the hydrodynamics of blood<sup>[10]</sup>. This subverts the previous understanding of mechanical signals and widens the impact of the mechanical microenvironment on cells.

Simple mechanical cues have been added into the culture requisites in tissue engineering for a better harvest. An example is the relocation of tissue engineering labs from rigid two-dimensional (2D) petri dishes to soft three-dimensional (3D) biomaterials, as the spatially constrained microenvironment and mechanical properties of 3D biomaterials are closer to those of *in vivo* tissues<sup>[11]</sup>. *In vitro*, the effects of mechanical signals may be easier to observe but may also be neglected due to simplified conditions. Therefore, it is still a challenge to simulate and regulate cell mechanical microenvironment in a precise manner.

3D bioprinting is a promising manufacturing method for precise control of the cell microenvironment<sup>[12]</sup>. Droplet-based bioprinting, laser direct-writing, extrusion-based bioprinting, stereolithography, and two-photon polymerization are the common types of 3D bioprinting. The 3D bioprinting technology is well developed for the fabrication of fine structures, thus enabling researchers to construct fine and complex structures. Besides the structure,

each bioprinting technique must be paired with specific biomaterials, which are known as bio-inks. Some of the common combinations are as follows: low-viscosity liquid materials for droplet-based bioprinting, donor substrate for laser direct-writing<sup>[13]</sup>, shear-thinning materials for extrusion-based bioprinting<sup>[14]</sup>, and liquid photocurable materials for stereolithography and two-photon bioprinting<sup>[15]</sup>. Regardless of the technique, the primary role of bio-inks for living cells is the same; that is, as a substitute for ECM, thus providing a controllable microenvironment for cells. An ideal bio-ink should provide cells with a living environment comparable to that of the ECM.

Currently, there is no bio-ink that can fully mimic the ECM, especially in the mechanical microenvironment. Given the diversity and potent modification potential of bio-inks, this goal remains achievable in the future. Bio-inks have been recognized as vital vehicles for the modulation of cell mechanical microenvironment in 3D bioprinting. To date, some well-written review papers on bio-inks have been published with a focus on biofabrication techniques or biological applications<sup>[12,16]</sup>. However, to the best of our knowledge, there is no comprehensive summary of the engineered bio-inks used for 3D bioprinting of cell mechanical microenvironment. Herein, we summarize the typical mechanical microenvironment of cells, which was used as a standard to compare the mechanical properties of existing engineered bio-inks, as well as characterize and propose some methods for ink selection. Following that, we discuss the limitations of previous studies and suggest several future research directions.

## 2. Cell mechanical microenvironments

In order to simulate the cell microenvironment *in vitro*, it is necessary to use the *in vivo* state as the standard and reference. It is also essential to understand the mechanisms by which cells sense their microenvironment. As parenchyma, cells can passively withstand various external mechanical stimuli and transmit mechanical signals to the nucleus through the cell membrane and/or cytoskeleton to regulate cell behaviors (a process termed as mechanotransduction)<sup>[17]</sup>. Besides, cells can also sense the mechanical microenvironment through the cytoskeleton or by forming mechanical interaction with the microenvironment. The cytoskeleton is an intracellular reticular organelle that is widely distributed in the cell, and it consists of one of its three distinct subunits; i.e., F-actin, microtubules, and intermediate filaments<sup>[18]</sup>. The regulation of the cytoskeletal network affects the mechanical properties of cells, which in turn influence cell division, differentiation<sup>[19]</sup>, and motility<sup>[20]</sup>. The cytoskeleton itself has a certain mechanical strength and maintains the cell shape when the cell is deformed<sup>[21]</sup>. It

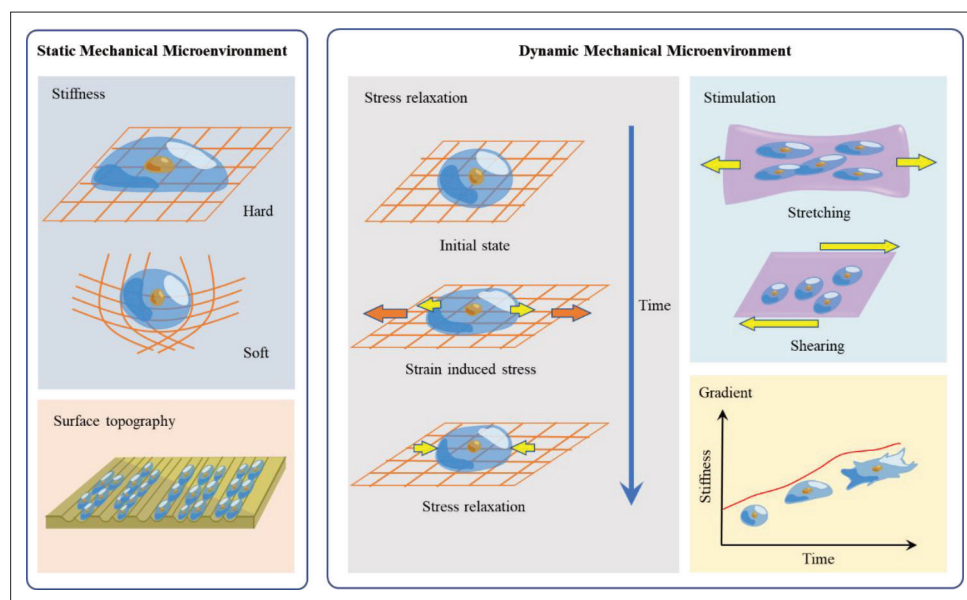


**Figure 1.** Bio-inks for bioprinting cell mechanical microenvironment mimicking the native microenvironment. Engineered cell mechanical microenvironment with bio-inks can be classified into two types: static and dynamic. Common static mechanical microenvironments include stiffness and surface topography; matrix stiffness affects a single cell's spreading, while surface topography regulates alignment. Common dynamic mechanical microenvironments include stress relaxation, mechanical stimulation, and gradients; stress relaxation is a state in which strain is maintained and stress decreases over time; tensile or shear forces from different directions are applied in dynamic mechanical stimulation; stiffness gradients can alter cellular behavior over time and space.

also provides a scaffold with increased surface area for the motor proteins<sup>[22]</sup>, so that these proteins can be transported on it to govern cell movement or generate internal stress. Through the cytoskeleton, cells are connected to the outside world (neighboring cells or ECM network), and they can deform, depolymerize, and reorganize in response to changes in the mechanical microenvironment, resulting in noticeable changes in gene expression.

In recent years, there has been a discovery of several mechanical signaling pathways, involving yes-associated protein/transcriptional coactivator with PDZ-binding motif (YAP/TAZ) activity<sup>[23]</sup>, Lamin<sup>[24]</sup>, and myocardin-related transcription factors family<sup>[25]</sup>, which are affected by matrix stiffness, cell density, or dynamic stretch and shear. Changes in the mechanical microenvironment may alter the cytoplasmic nuclear translocation of the effector molecules, thereby affecting cell proliferation and differentiation<sup>[26]</sup>. Several diseases have also been found related to the dysregulation of mechanical signaling pathways. For instance, mutations in protein dystrophin that provides mechanical balance to muscle cells may lead to muscular dystrophy<sup>[27]</sup>. However, it is still unclear whether and how the mechanical signals in the microenvironment synergistically regulate cell behaviors. Engineering cell mechanical microenvironment *in vitro* that recapitulates the native microenvironment will be beneficial to researchers in clarifying how tissue

engineering can benefit from modulating mechanical signaling. The mechanical cues in cell microenvironment include stiffness, viscoelasticity, surface topography, and dynamic mechanical stimulation (Figure 1).

## 2.1. Stiffness

Stiffness is a material mechanical concept that reflects the ability of an object to resist deformation under an applied force. In the elastic range, stiffness is usually determined by the ratio of the applied force to the displacement produced by the force along the same direction. For most solid materials, stiffness is widely applicable to a given structure. Since many objects are anisotropic (exhibiting different properties in different degrees of freedom), stiffness is a structure- and boundary-dependent property that characterizes the macroscopic mechanical properties of materials. Another measurement unit of an object's ability to resist elastic deformation is the elastic modulus, which is defined as the ratio of stress to the strain of an object in the elastic deformation region. According to different stress and strain directions, the elastic modulus can be divided into Young's modulus ( $E$ , tensile stress and tensile strain) and shear modulus ( $G$ , shear stress and shear strain).

In a strict sense, the definition of stiffness is inseparable from structural conditions and is used to characterize the macroscopic structure rather than the properties of the material itself. The elastic modulus reflects the

**Table 1. Stiffness values of living tissues at different scales**

Tissue	Modulus	Modulus value	Dimension	Test mode	Refs.
Bone	<i>E</i>	1.28–1.97 GPa	Nanoscale	AFM	[36]
Bone	<i>E</i>	10.4–20.7 GPa	Macroscale	USE, Micro-tensile	[29]
Cardiac muscle	<i>E</i>	8 kPa	Macroscale	MRE, Tension	[84]
Cardiac muscle	<i>G</i>	5–50 kPa	Macroscale	USE, MRE	[85]
Lung	<i>G</i>	0.84–1.5 kPa	Macroscale	MRE	[86,87]
Lung	<i>E</i>	1.96 kPa	Nanoscale	AFM	[88]
Liver	<i>E</i>	1.5–6.5 kPa	Macroscale	USE, Cyclic compression-relaxation	[89–91]
Liver	<i>G</i>	2 kPa	Macroscale	MRE	[92,93]
Liver	<i>E</i>	162–248 kPa	Macroscale	Probing (Entire organ)	[94]
Pancreas	<i>E</i>	2.8 kPa	Macroscale	USE	[95]
Pancreas	<i>G</i>	1.11 kPa	Macroscale	MRE	[96]
Kidney	<i>E</i>	1–2 kPa	Nanoscale	Nanoindentation	[74]
Kidney	<i>E</i>	35.3–68.9 kPa	Macroscale	Probing (Entire organ)	[94]

Abbreviations: AFM, atomic force microscopy; *E*, elasticity modulus; *G*, shear modulus; MRE, magnetic resonance elastography; USE, ultrasonic elastography.

properties of the material itself, which is independent of shape and structure. However, given the inseparable complexity of biomaterials (especially polymeric materials and anisotropic biological tissues), the “stiffness” for biomaterials in research is often characterized using modulus (e.g., elastic modulus). In many studies, although a piece of tissue may contain both, dense fibers and loose matrix at the molecular (microscale) level, it is still measured as a whole, without considering the uneven distribution of matter at a smaller scale.

Living tissues have a wide range of stiffness, especially in higher animals with more complicated structures, such as the intuitive difference in stiffness between a “hard” bone and a “soft” brain<sup>[28]</sup>. Comparing only in terms of elastic modulus, the elastic modulus of bone is as high as 20 GPa<sup>[29]</sup>, while that of mucus is only 11 Pa<sup>[30]</sup>. The specific functions of distinct organs determine the variances in stiffness of living tissues (e.g., weighed bone has the highest stiffness of all tissues), and the cells within the matrix have specialized interactions with the stiffness microenvironment. The stiffness of abnormal tissues also has its own specificity. For instance, there is significant difference in tumor stiffness among liver malignancies, with cholangiocellular carcinoma (75 kPa) being stiffer than hepatocellular carcinoma (55 kPa) and metastatic tumors (66.5 kPa)<sup>[31]</sup>. This stiffness difference may provide the basis for clinical diagnosis. It is also worth noting that cell stiffness differs from tissue stiffness. Although bone has a stiffness of 20 GPa, the stiffness of osteoblasts, which are cells that synthesize bone, is only 2.6 kPa (unspread spherical) or 6.5 kPa (spread)<sup>[32]</sup>. Hard bone is the result of the accumulation and mineralization of ECM and the

bone’s porous 3D structure enhances the overall system’s stiffness<sup>[33]</sup>.

It is worth noting that although most studies provide specific values for tissue stiffness, there is no gold standard test for measuring stiffness in biological tissues. Stiffness values in tension (elastic modulus), compression (elastic modulus), and shear (shear modulus) are likely to differ for bulk structures, and tests for surface stiffness (indentation test) may provide different stiffness values. For cellular stiffness, measurements by atomic force microscopy (AFM)<sup>[34]</sup> and optical tweezers<sup>[35]</sup> are commonly used. This leads to significant differences between the macroscale and microscale stiffness of the same material. When bone tissue is measured at the microscopic scale, it may only show a stiffness of 1.97 GPa<sup>[36]</sup>, which differs from the macroscopic result. Living tissue *in vivo* is usually measured using elastography (Table 1). Table 1 shows the stiffness values measured by different methods for certain living tissues in the human body.

Different organs or tissues have specific structures, owing to the uneven distribution of internal substances. For example, more fibers confer elasticity to blood vessel walls. The renal cortex has more blood vessels than the renal medulla. This macrostructure has a decisive influence on the overall mechanical property. According to Table 1, intact livers and kidneys have high compressive moduli, allowing them to withstand certain shocks without damage. However, in micromechanical tests, in which organs are cut into small samples, they show mechanical properties on the order of magnitude of lungs. By eliminating the effects of part of the macrostructure, seemingly dissimilar

tissues show partially similar mechanical properties, resulting in dramatic changes. Similar differences have been observed in various *in vivo* and *in vitro* experiments that were cell-contained and decellularized. Although these vastly different values cannot be converted, they are not contradictory findings, but rather a reflection of the diversity in mechanical properties of the same tissue under controlled conditions.

The stiffness of the cell microenvironment is a dynamic factor that varies with cellular activity over time. The deposition of ECM, which is a dynamic network, occurs during physiological processes as a result of cellular activity and influences cellular behavior. The conversion of cartilage to bone is a complex equilibrium by regulating the turnover and remodeling of ECM<sup>[37]</sup>. This process involves multiple ECM-related components and is continuously dependent on the stiffness of ECM<sup>[37]</sup>. Abnormal ECM stiffness leads to the occurrence and progression of the disease. For instance, a rigid ECM may engender the transformation of normal epithelial cells into cancer cells, increase tumor aggressiveness, and prevent drug penetration into the tumor interior<sup>[38]</sup>. Cells also exhibit dynamic stiffness during various stages of their life cycle, and the variations in ECM stiffness that accumulate over time can be monitored and may alter gene expression. Primary human epithelial cells were passaged with increased stiffness on plastic petri plates, with cell stiffness rising two to four times after eight passages compared to cells passaged less than three times<sup>[39]</sup>. With increasing passage number, the endometrial adenocarcinoma cells grown on plastic petri plates showed a transition to the stromal phenotype, along with an increase in  $\alpha$ -actin expression<sup>[40]</sup>. Dynamic stiffness increases the variables in studies, which undoubtedly heightens the complexity of tissue engineering *in vitro*.

## 2.2. Viscoelasticity

Besides stiffness, biological tissues have other notable mechanical properties. The water content of immature brain tissue is more than 80%, while that of normal liver is about 65%<sup>[41]</sup>. When water takes up a significant amount of space in tissues, its flow properties must be considered. This is known as viscoelasticity. The material in this situation has both, solid and fluid features. Viscoelasticity is characterized by the combination of viscosity and elasticity or the flow properties of viscous fluids and elastic solids.

Viscoelasticity is a property of most living tissues and polymer hydrogels that manifest as partly elastic and viscoplastic. It is a dynamic mechanical microenvironment in the temporal sense. While a material is subjected to moderate stress, it tends to return to its original shape, owing to elasticity. However, viscoplasticity prevents

it from fully returning to its original shape after being subjected to excessive stress; the internal stress of the material progressively reduces over time (known as stress relaxation). Viscoelasticity is determined by the movement of polymer chains. As a result, it is influenced by a variety of variables, including temperature, stress, strain, frequencies, test time, and orientation. The characterization of viscoelasticity must be dynamic, applying programmed strain over some time and measuring the response stress as a function of time, or applying stress and measuring strain as a function of time. Programmatic temperature changes and frequency can also be used as variables, but they must be time-dependent.

The dual properties of viscoelastic materials must be characterized by a complex modulus, which is typically the storage modulus and loss modulus. The storage modulus represents the elastic property of materials, which is the ability to instantaneously recover from deformation. It can be divided into axial storage modulus ( $E'$ ) and shear storage modulus ( $G'$ ) according to the direction. On the other hand, the loss modulus represents the viscous property of materials, which is the ability to irreversibly remodel over time. It can also be divided into axial loss modulus ( $E''$ ) and shear loss modulus ( $G''$ ). In viscoelastic testing, the storage modulus and loss modulus are two functions of time. When the storage modulus is significantly more than the loss modulus, the material is regarded to be solid; when the loss modulus is much greater than the storage modulus, the material is thought to be liquid; and when the storage and loss moduli are comparable, the material is said to be gel.

Stress relaxation is a common viscoelastic behavior in living tissues, which can occur in ECM. It plays an important role in tissues subjected to periodic loads, such as cartilage, tendons, skin, and alveoli<sup>[42]</sup>. More recent studies have demonstrated that the stress relaxation of ECM affects not only cell differentiation<sup>[43]</sup>, but also cell spreading<sup>[44]</sup> and migration<sup>[45]</sup>. The storage part of the cell deformation stress in the substrate is countered by the stress relaxation of living tissue, which prevents cells from being continuously restrained when stretched, thus resulting in a continuously changing dynamic effect on the cells. However, the overall effects of stress relaxation on cells remain unclear; hence, the optimal viscoelastic parameters for different tissue engineering have yet to be investigated.

## 2.3. Surface topography

Surface topography is a concept that extends from 2D to 3D. This concept was originally described on 2D cultured surfaces. The surface features of scaffold expansion are also of relevance as cell culture progresses to 3D scales. Surface

topography is often studied in instances where cells need to be attached and proliferate, such as in the implantation of metal joints in the body or polymer scaffolds.

Roughness is one of the properties that characterize surface topography. It describes the measurable change in height of the material surface in a certain direction of the profile. Roughness can be detected at different scales using a stylus profilometer (0.1  $\mu\text{m}$ )<sup>[46]</sup>, an AFM (0.01 nm) probe<sup>[47]</sup>, or an optical apparatus (non-contact, resolution depends on wavelength)<sup>[48]</sup>. This property can be observed with a scanning electron microscope<sup>[49]</sup>. When the roughness is isotropic, unstructured, or nearly randomly distributed, the increased roughness at the macroscale will affect the wettability of the material, making the material more easily wetted by body fluids and adsorb proteins, thus promoting cell adhesion<sup>[50]</sup>. However, for cells, microscopic adhesion does not depend on the surface height; instead, the molecular composition of the material is more important than the smoothness of the surface. For example, it is difficult for cells to attach to polyethylene glycol (PEG) hydrogels without the modification of arginylglycylaspartic acid (RGD peptide), no matter how rough the surface is<sup>[51]</sup>.

If the roughness is anisotropic, structured, or regular, it can be considered as a pattern. Reasonably designed patterns can regulate cell behaviors; for instance, groove patterns can regulate the alignment of cells<sup>[52]</sup>, which plays an important role in engineering microenvironments with anisotropic characteristics (e.g., cardiac cells and neurons)<sup>[53]</sup>. Cells prefer to grow along the long axis of the groove rather than spanning<sup>[54]</sup>, which may be related to the slope distribution of the topography and the deformation of the cytoskeleton.

#### 2.4. Dynamic mechanical stimulation

At the macroscale, the majority of dynamic mechanical stimulations based on the mechanical microenvironment are used to mimic the motion of genuine living tissues, such as the stretching of skeletal muscle, the shearing of cartilage, and the tension of skin for scar tissue formation. For instance, a stretch pattern of 25% stretch at 12-s intervals for 12 to 36 h resulted in a considerable activation of skeletal muscle satellite cells<sup>[55]</sup>. This is essential for muscle repair and regeneration. Induced mechanical shearing of synovial fluid with cartilage during joint movement promptly activates latent transforming growth factor-beta, which affects the biosynthesis of chondrocytes<sup>[56]</sup>. For the skin environment, restrictions on skin stretching can slow the formation of keloids, as the incidence of keloids increases with skin tension, especially in cyclically stretched body parts<sup>[57]</sup>.

When we focus on dynamic mechanical stimulation at the microscale, the microenvironment may become

complicated. Mechanical stimulation to the material often causes displacements that may lead to simultaneous changes in various dimensions. The sliding of molecular chains caused by material stretching changes the relative positions of cell attachment sites. The shift in the attachment sites deforms the cell membrane and skeleton, potentially generating mechanical signals. However, many living tissue matrices have stiffness that varies with stress, such as collagen and fibrin, whose substantial increase in stiffness following stress exceeds a critical value (i.e., stress stiffening). These changes in stiffness can also be detected by cells<sup>[58]</sup>. It is difficult to distinguish the factors that influence cell activities while attempting to refine the studies in view of the multiple mapping results that correspond to one stimulus. Alike stress relaxation, dynamic mechanical stimulation is a multidimensional time-dependent environment.

### 3. Properties of bio-inks

Biomaterials used in 3D bioprinting can be classified as hydrogel bio-inks and non-hydrogel scaffold materials. Scaffold materials are pre-prepared and molded materials for cells to attach to, whereas bio-inks are encapsulated and printed with living cells. Both, scaffolds and bio-inks have basic biocompatibility, which allows cells to thrive. The mechanical properties of materials are determined by the polymer backbone as the main component and the intermolecular bonds, which can be covalent, ionic, and/or hydrogen bonds, in addition to spatial topology. We summarized the mechanical properties (range of modulus values) of several commonly used bio-inks under different conditions (Table 2). In fact, the mechanical properties of materials are affected by various factors. There are now more mechanical properties to choose from for materials, and their combinations and derivatives are constantly being developed, making it easier to mimic native cell mechanical microenvironment. Since 3D bioprinting has been extensively discussed as a standardized and common means of biofabrication in many works, we will not go into detail about 3D bioprinting. In order to ensure a focused discussion, this review may pay attention to materials for extrusion-based bioprinting and stereolithography based on commonality and functionality.

#### 3.1. Hydrogel bio-inks

Almost all bio-inks contain hydrophilic macromolecules as the main chain in order to mimic the properties of ECM as closely as possible and improve biocompatibility. As a result, bio-inks are in a hydrogel state following cell loading. Bio-inks are available in a wide range of materials, but most of them are used for extrusion-based 3D bioprinting due to shear-thinning rheology. Those that can be modified with photocurable groups and have

Table 2. Stiffness values of bio-inks at different scales

Material	Modulus	Modulus value	Dimension	Test mode	Condition	Concentration (w/w)	Refs.
<b>MW</b>							
PEGDA	<i>E</i>	6.5–30 MPa	Nanoscale	AFM	700 Da	*	[97]
	<i>E</i>	36 kPa	Macroscale	Compression	2000 Da	15.0%	[98]
	<i>G</i>	10 kPa	Macroscale	Compression	2000 Da	15.0%	
	<i>E</i>	200–400 kPa	Macroscale	Tension	3000 Da	20.0%	[99]
	<i>E</i>	40 kPa	Macroscale	Tension	6000 Da	5.0%	[100]
	<i>E</i>	200 kPa	Macroscale	Tension	6000 Da	10.0%	
	<i>E</i>	320 kPa	Macroscale	Tension	6000 Da	15.0%	
	<i>E</i>	430 kPa	Macroscale	Tension	6000 Da	20.0%	
<b>Temperature</b>							
GelMA	<i>E</i>	133 kPa	Nanoscale	AFM	25°	10.0%	[101]
	<i>E</i>	171 kPa	Nanoscale	AFM	25°	20.0%	
	<i>E</i>	2.86 ± 0.1 kPa	Macroscale	Compression	25°	5.0%	[102]
	<i>E</i>	2.41 ± 0.38 kPa	Macroscale	Compression	37°	5.0%	
	<i>E</i>	288.24 ± 62.34 kPa	Macroscale	Compression	25°	30.0%	
	<i>E</i>	216.81 ± 10.28 kPa	Macroscale	Compression	37°	30.0%	
	<i>E</i>	2.08 ± 0.43 kPa	Macroscale	Tension	25°	5.0%	
	<i>E</i>	1.67 ± 0.56 kPa	Macroscale	Tension	37°	5.0%	
	<i>E</i>	264.74 ± 11.08 kPa	Macroscale	Tension	25°	30.0%	
	<i>E</i>	226.80 ± 39.97 kPa	Macroscale	Tension	37°	30.0%	
Agarose	<i>E</i>	168 kPa	Nanoscale	AFM	25°	1.00%	[101]
	<i>E</i>	230 kPa	Nanoscale	AFM	25°	2.00%	
Alginate	<i>G</i>	0.203 ± 0.013 kPa	Macroscale	Compression	20°	0.70%	[103]
	<i>G</i>	1.300 ± 0.129 kPa	Macroscale	Compression	20°	1.50%	
	<i>G</i>	3.010 ± 0.084 kPa	Macroscale	Compression	20°	3.00%	
Collagen (Type I)	<i>E</i>	~200 Pa	Nanoscale	AFM	20°	0.20%	[104]
	<i>E</i>	~500 Pa	Nanoscale	AFM	20°	0.30%	
	<i>E</i>	~800 Pa	Nanoscale	AFM	20°	0.40%	

Abbreviations: AFM, atomic force microscopy; *E*, elasticity modulus; *G*, shear modulus; MW, molecular weight. \*Poly(ethylene glycol) diacrylate (PEGDA) of this molecular weight is liquid.

suitable gel stiffness are used in stereolithography. There is no complete division of the materials used in these two bioprinting methods. Poly (ethylene glycol) diacrylate and gelatin methacryloyl (GelMA), for example, are competent for both fabrication methods.

Bio-inks can be divided into two types according to the source: natural and synthetic bio-inks. Alginate (from brown algae), agarose (from red algae), chitosan (from shrimp shells), silk fibroin (from silk), gellan gum (from microbial fermentation), cellulose (from plant stalks), collagen (from animal tendon), gelatin (from collagen), fibrin/fibrinogen (from plasma), hyaluronic acid (from cartilage), and mixed components of decellularized ECM are some of the major natural inks. Polymer macromolecules such as PEG, pluronic, and polyacrylamide (PAAm) are

examples of synthetic bio-inks. Natural and synthetic materials can complement each other, with no clear-cut advantages or disadvantages. The main skeletons of natural inks often contain reactive groups, such as hydroxyl and amino groups, making them easily chemically modifiable. Synthetic inks, on the other hand, have a more controllable structure and can be programmed to form more complex materials (e.g., star-shaped PEG polymers)<sup>[59]</sup>.

Natural hydrogel sources are not always more biocompatible than synthetic ones; in fact, animal protein sources and species-antigen relationships are important factors in determining biocompatibility. Alginates from nature, for example, do not always have better performance than synthetic hydrogels at cell adhesion, and in order to be suitable for cell spreading, both require covalent

modification. The content of proline and hydroxyproline in fish gelatin is lower than that of pork gelatin, but the content of threonine and serine is higher<sup>[60]</sup>. The differences in amino acid and peptide compositions can affect spatial conformation and confer different mechanical properties to biomaterials derived from different sources.

The mechanical properties of bio-inks are also determined by the arrangement and assembly of molecules. In view of its highly ordered spatial structure, collagen imparts extremely high mechanical properties to tendons and ligaments<sup>[61]</sup>. Despite being derived from tendons, *in vitro* collagen hydrogel fabrication based on pH and irreversible chemical cross-linking (e.g., genipin) cannot replicate the high strength of native tendons<sup>[61]</sup>. Similar problems arise in ECM extracts, such as Matrigel, whose gel strength is an order of magnitude lower than ideal materials and is greatly influenced by the donor source<sup>[62]</sup>.

### 3.2. Non-hydrogel bio-inks

Most hydrogel bio-inks can either encapsulate cells or act as adhesive scaffolds. This section only discusses non-hydrogel materials for scaffolds. Typically, such materials cannot be loaded with cells because the manufacturing process of scaffold is unsuitable for cell survival. As a result, they are not always discussed in conjunction with bio-inks. However, as the performance of extrusion-based bioprinters has improved in recent years, some scaffold materials can be processed together with bio-inks. Also, the fact that scaffold materials play an inseparable role in the mechanical microenvironment is important.

Aliphatic polyesters are considered a type of scaffold material that is commonly used in 3D bioprinting. They have become one of the most widely used biopolymers in the biomedical field due to their non-toxicity, biodegradability, and good biocompatibility. Natural compounds such as lactide, glycolide, and  $\epsilon$ -caprolactone are used to make aliphatic polyesters<sup>[63]</sup>. Common polyesters are polylactic acid, polyglycolide (PGA), poly( $\epsilon$ -caprolactone) (PCL), poly( $\gamma$ -valerolactone), polydioxone (PDO), and their copolymers, such as poly(lactic-co-glycolic acid) (PLGA). The ester functional groups in the (co)polymer backbones of aliphatic polyesters can be hydrolyzed by enzymes, resulting in water and carbon dioxide as degradation products<sup>[64]</sup>. This means that aliphatic polyesters can be eroded by cells.

Aliphatic polyesters are thermoplastic and can be formed into highly precise structures using the printers' controlled extrusion. The temperature of fabrication varies by composition and molecular weight, with relatively controllable rates of degradation. The melting point of aliphatic polyesters increases with crystallinity, and their degradation rate decreases with hydrophilicity, which also affect their mechanical properties<sup>[65]</sup>. Semi-crystalline

PCL, for example, has a slow degradation rate. The copolymerization of PCL with other monomers can meet the requirements for optimally controlled mechanical properties in tissue engineering<sup>[63]</sup>. When PCL is combined with PLGA copolymers, the degradation rate increases.

It takes time for cells to adhere to and spread on the scaffold material. Using cell-loaded bio-inks and collaborating with the scaffold would not only temporarily fix the cells' spatial position in case of loss, but also mimic the solid-liquid bidirectional microenvironment at the junction of certain tissues.

## 4. Basic mechanical microenvironment and bio-inks

As a substitute for ECM *in vitro*, the performance of bio-ink should be compared with the cell microenvironment *in vivo* as a standard. Therefore, in *in vitro* experiments, the mechanical properties of bio-ink themselves are as important as the matrix mechanical microenvironment. In current research context, the mechanical characterization of living tissue is applicable in the mechanical microenvironment of bio-inks, such as stiffness, stress relaxation, etc.

### 4.1. Static mechanical microenvironment

Static mechanics are basic conditions that do not change with time. The static mechanical microenvironment, as a highly researched mechanical cue, is relatively easy to realize. As the most basic, initial stiffness is a fairly controllable variable, in which many natural or synthetic polymer materials can perform this task well.

Osteocytes require a microenvironment with high initial stiffness, in particular, the differentiation of osteoblasts. For environments with high initial stiffness, aliphatic polyesters, such as PCL, polylactic acid, PGA, and PDO, which are printed by high-temperature extrusion and have modulus with GPa level, allow the approximation of the stiffness of bone tissue and cell adhesion without modification<sup>[66]</sup>. These materials have different mechanical properties and degradation rates according to the variation in composition and molecular weight. In general, PGA has a higher stiffness (>7 GPa), while PDO is relatively soft (1–2 GPa)<sup>[66]</sup>. During bioprinting, due to their similar thermoplastic properties, aliphatic polyesters can be mixed in different proportions as required, blended with other functional components, or chemically modified to achieve different molding conditions and specific needs. When simulating bone tissue, structural design is as important as material stiffness. According to studies, the hardness of cancellous bone is 12% less than that of adjacent compact bone; this is not entirely due to content difference<sup>[67]</sup>. Stiffness tests in various directions are required, owing to

the influence of structures on the mechanical strength of compact and cancellous bone.

Materials for high-temperature bioprinting cannot be loaded with cells, and hydrogel bio-inks are required if a 3D-wrapped matrix environment is needed. Synthetic polymer hydrogels such as PEG and PAAm, natural polymer hydrogels such as chitosan, gelatin, and alginate, as well as chemically modified semi-natural hydrogels such as GelMA and hyaluronic acid methacryloyl (HAMA) can be used as the main components to simulate the initial stiffness. According to the specific needs in bioprinting, the polymer main skeleton can be chemically modified. With the exception of ECM-derived hydrogels (e.g., collagen, gelatin, fibrin, and GelMA), most polymer hydrogels lack cell adhesion sites (bioinert). Hence, if they are not chemically modified (such as RGD peptides) or mixed with ECM analogs, cells are unable to transmit mechanical signals to the cytoskeleton through adhesion sites even if the stiffness is similar, thus behaving in an abnormal state.

The initial stiffness of hydrogels is controlled by the concentration and degree of cross-linking. Generally, increasing the concentration of substances in hydrogels can increase the stiffness, thus providing an easier substrate for cells to attach to. Increasing the cross-linking density of gel can also increase the stiffness while maintaining the same substance concentration. For example, GelMA with a 96% degree of substitution has a Young's modulus of 3.08 kPa at a concentration of 5%, which increases to 184.52 kPa at a concentration of 30%<sup>[68]</sup>. The same 10% concentration of GelMA hydrogel has a compressive Young's modulus of 9.23 kPa with 81.3% degree of substitution, but only 5.66 kPa for the hydrogel with 41.6% degree of substitution. This indicates that increasing the degree of substitution can increase the cross-linking density<sup>[69]</sup>.

There are limitations to the microenvironment stiffness raised by the concentration and cross-linking density. Since the spreading and movement of cells depend on the space between the molecular chains in the hydrogel, the living space of the cells would be limited if the substance concentration is too high. This would in turn lead to problems in cell growth and proliferation. Developing the double-network system, which comprises two hydrogels with separate elastic networks, is one way to overcome this constraint. After cross-linking, the two networks nest inside each other, enabling sliding when deformed and conferring the total system a larger elastic modulus with better mechanical properties than the two single-network hydrogels. GelMA, for example, can be stiffened on modulus by adding low amounts of HAMA (1% w/v), and its mechanical properties are superior to monohydrogel systems with high concentrations<sup>[70]</sup>.

#### 4.2. Surface topography

Surface topography or patterning is also a basic microenvironment that necessitates both stiffness and fabrication precision control. In this regard, stereolithography has an advantage over extrusion-based bioprinting due to its higher resolution. There will be higher resolution for profile height with smaller layer heights. The most important initial factor affecting the structural resolution is the swelling of bio-inks, which is an equilibrium process of two opposite trends. Volume expansion occurs as a result of the penetration of solvent into the hydrogel network, leading to the extension of the 3D molecular network and the polymer chain between the cross-links, which reduces its conformational entropy; the elastic contraction force of the molecular network then attempts to shrink the network. Except for solid scaffolds, all hydrogels swell at varying degrees after immersion, making the grooves and ridges disappear, and reducing the resolution of patterns and blurring boundaries. The network dilution caused by the swelling behavior leads to a dramatic decrease in the mechanical strength of the hydrogel<sup>[71]</sup>. Hence, bio-inks with a low swelling ratio are preferred<sup>[72]</sup>, and swelling strengthening hydrogels using embedded networks is also an effective solution to this<sup>[73]</sup>.

#### 5. Complex mechanical microenvironment and challenge for bio-inks

Real living tissue is far more complex than a hydrogel with fixed stiffness. When controlling one of these cues, the conditions in other dimensions tend to vary from the optimum, especially for living tissue, such as the flaws in plasticity in high stiffness materials, a lack of stress relaxation that may confine cells, and so on. In the current field of research, this is an unsolved challenge. As a result, most studies focus on mechanical microenvironments with a narrow range of factors, while other distortions are omitted. Occasionally, these omissions are acceptable for research progress. It is possible to have multiple design strategies for a particular mechanical microenvironment, and comparable aims can be achieved with the use of diverse bioprinting materials, which is not constrained to a single solution.

##### 5.1. Anisotropic mechanical microenvironment

A shared disadvantage of commonly used bio-inks is the mismatch between their mechanical properties and isotropy with *in vivo* tissues. Unlike natural tissues with uneven distribution, bio-inks lack anisotropy and complexity. They are unable to exhibit the diverse mechanical properties of living tissues at different scales even with the fabrication of similar structures. Considering the differences in the mechanical microenvironment of living tissue at various scales, there will be many challenges encountered when designing and

simulating these microenvironment cues. Although many researchers have claimed that their models and materials are accurate replicas of a certain microenvironment, no *in vitro* model has yet to match the mechanical cues of living tissues. Native tissues have microstructures that give them distinct mechanical properties in different directions; for instance, myocardium-specific microstructure endows the heart with anisotropic modulus, thus conferring the heart with significant directional properties during contraction<sup>[74]</sup>. Reproducing this anisotropy *in vitro* has become a challenge for cardiac regenerative medicine. Achieving this anisotropy through non-uniform bio-ink arrangement is one of the directions for future research on cell microenvironment.

The mixing of multiple bio-ink components allows for partially anisotropic microenvironments. In order to exhibit different stiffness distributions in the same space, it is necessary to create a gradient stiffness structure. The gradient of stiffness can be regulated by either a concentration gradient or a cross-linking degree gradient. Coaxial bioprinting or multi-jet bioprinting is useful for gradient structures<sup>[75]</sup>, and by adjusting the bio-ink input or curing parameters, a layer-by-layer gradient environment can also be achieved via lithography. For example, soft hydrogels are mixed with stiff hydrogels in dynamic ratios during bioprinting by a static mixer device, resulting in a graded stiffness gradient (Figure 2)<sup>[75]</sup>. In a

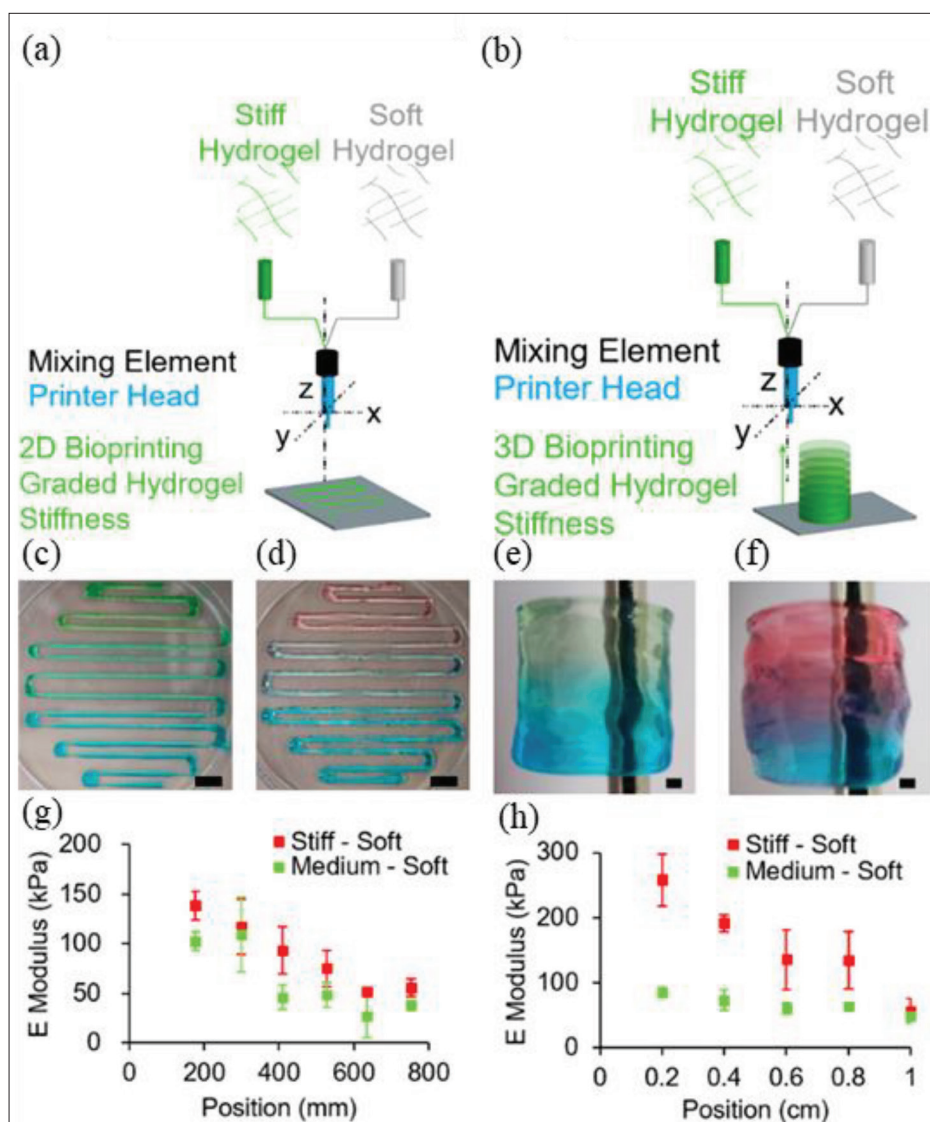


**Figure 2.** Extrusion bio-inks for engineering stiffness gradient microenvironment. Scheme depicting the bioprinting experiment of (A) two-dimensional (2D)- and (B) three-dimensional (3D)-graded stiffness. The colored gels reveal the changes in hydrogel compositions from (C, E) stiff (red) to soft (blue) and (D, F) medium (green) to soft (blue). The mechanical properties of (G) 2D and (H) 3D prints have been analyzed by indentation tests; the E modulus equals the indentation elastic modulus. Error bars show a standard deviation of  $n = 3$ . Scale bars: (C, D) 10 mm, (E, F) 1 mm<sup>[75]</sup>.

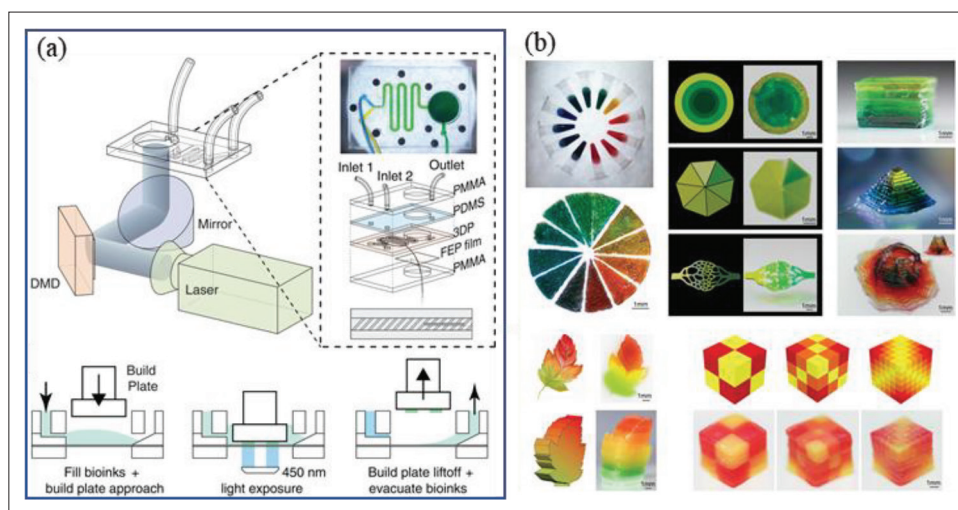


**Figure 3.** Stereolithography bio-inks for engineering stiffness gradient microenvironment. (A) A schematic diagram of ink mixing controlled by a microfluidic chip. (B) Mixing three colored poly(ethylene glycol) diacrylate (PEGDA) inks to obtain continuous gradient colors for printing two-dimensional (2D) and three-dimensional (3D) gradient structures<sup>[76]</sup>.

recent study, composable gradients of stereolithography were achieved by using a microfluidic chip to control the mixing of bio-inks of different components (Figure 3)<sup>[76]</sup>. The multiple printing of different bio-inks can increase the scale of complex structures. For example, cells are loaded into bio-inks to make gel microfibers, and after mixing, the microfibers are aligned by secondary extrusion, thereby obtaining the directional arrangement of cells. The utilization of these bio-inks can partially resolve the anisotropy of the mechanical microenvironment, but further studies are still required for more precise control, which may be solved by dynamic regulation<sup>[77]</sup>.

## 5.2. Dynamic mechanical microenvironment

When structures and cells are co-cultured, the initial stiffness gradually changes over time, resulting in a temporal stiffness gradient. As a general rule, bioactive bio-inks are degraded by cells in a gradual manner, and the loss of mass due to degradation inevitably reduces stiffness. On the other hand, cells proliferate while secreting ECM to deposit on the scaffold and changing the matrix's mechanical properties. This process is called ECM remodeling<sup>[78]</sup>. The rate of degradation can be controlled by material design, while remodeling depends on the state of cells and tissues<sup>[79]</sup>. Remodeling and degradation usually occur simultaneously, and their synergistical effects determine the temporal change of the mechanical microenvironment. This process is both inevitable and difficult to control, and remains as one of the relatively uncharted territories of bio-inks.

Stress relaxation is another dynamic mechanical cue that can be simulated, and by tuning the material, it is possible to

achieve viscoelasticity independent of the initial stiffness. This feature is particularly important in studying stem cell differentiation and the mechanical microenvironment of cancer cells. According to preliminary studies on stress relaxation of bio-inks, cross-linked covalent bonds store pure elasticity, whereas weaker non-covalent bonds allow for some modulus dissipation<sup>[80]</sup>. Alginate is one of the commonly used materials to tune viscoelasticity due to its ionic cross-linking properties. In a study, alginate and PEG were covalently grafted together to achieve different stress relaxations by changing the molecular weight of PEG and the ionic cross-linking concentration of alginate<sup>[81]</sup>. The increase in PEG concentration and molecular weight resulted in faster stress relaxation, higher loss modulus, increased creep, and a significant impact on fibroblast proliferation and osteoblast differentiation<sup>[81]</sup>. In addition, this system can attenuate the interference of biodegradation on stiffness changes. Stress relaxation can also be achieved with interpenetrating network hydrogels based on HA-hydrazine and collagen. This combination has biocompatibility closer to native ECM than alginate<sup>[80]</sup>.

The dynamic mechanical stimulation of engineered cell microenvironment imposes requirements on bio-ink structures in addition to stiffness. It is necessary to ensure structural integrity throughout the dynamic mechanical stimulation loading cycle. Cyclic load testing, for example, requires a material with a suitable fatigue limit that can withstand a certain number of stretches or compressions without breaking or chipping. The non-hydrogel scaffold material has greater plasticity and is more prone to plastic deformation when bent. The fracture properties of hydrogels are affected by the cross-linking bond and

water content. It can be observed in PAAm that as its water content decreases, the gel becomes more brittle<sup>[72]</sup>. The mechanical reinforcement of brittle hydrogels through multi-network cross-linking or designing enhanced microstructures to improve compressive strength can help materials adapt to more dynamic mechanical tests.

## 6. Conclusion and prospect

Through the continuous research in recent years, a growing number of influencing factors of cell mechanical microenvironment have been uncovered and the principle has gradually become clearer. The use of bio-inks and scaffold materials to engineer cell mechanical microenvironment via 3D bioprinting has good feasibility and broad prospects for application, whether for mechanism exploration, drug testing as a disease model, or tissue regeneration simulation. Although it would be impractical to list out all of the application scenarios, a clear selection strategy can be obtained by summarizing the methods and experiences. First, it is important to identify which mechanical cues (stiffness, viscoelasticity, surface topography, or mechanical stimulation) in the native cell microenvironment we attempt to mimic in *in vitro* engineered cases. Then, the mechanical cues in native living tissues (as control) need to be examined, while determining the approximate range of its variables. Third, materials with mechanical properties similar to the target tissues should be selected. Finally, by optimizing the details (constants and variables), the simulated microenvironment would be able to mimic the native tissue.

However, from existing studies, the difficulty in horizontal comparison has always been an obstacle to repeated research and the accumulation of experiences. Whether on the macro or micro scale, either in tensile or shear directions, the variable that controls is critical and should be ensured to precisely match the research objectives. Rather than bulk stiffness, surface stiffness should be used as the standard of comparison when controlling variables for material surface adhesion. Young's modulus and shear modulus should not be compared horizontally, while AFM and rheometer results should not be compared in the same system either. When referring to stiffness experiments from other literature, the focus should be on the comparability of experimental methods. Mutually exclusive variables are also challenging for mechanical microenvironment simulation. For example, when matrix stiffness is controlled by concentration, the space of molecular chains changes, which virtually restricts the cell's movement and remodeling behavior. Moreover, the effect of macrostructure on the mechanical microenvironment is still unknown. The mechanical

differences exhibited by living tissues at different scales need to be further explained. Therefore, much research is still needed to determine whether the results, after disregarding these unknown quantities, can be used as a real response to the mechanical microenvironment.

Considering the limitations of the development of materials science, bio-ink materials are still far from being perfect in mimicking the properties of native ECM. They have poor stiffness tunability and different stress relaxations from natural tissues, which are not conducive for ECM remodeling in cells. In view of these disadvantages, a large number of uncontrollable factors have been disregarded by many studies. However, in recent years, with the emergence of four-dimensional bioprinting technology and the development of smart materials, materials that can actively change their mechanical properties, such as self-deforming printed structures<sup>[82]</sup>, are also increasing, and stiffness-adaptive dynamic-structure host-guest-macromer hydrogels, which are more favorable for cell motility, have also been identified<sup>[83]</sup>. These discoveries will inevitably expand the boundaries of *in vitro* stimulation of cell mechanical microenvironment and steadily advance simulation research.

## Acknowledgments

None.

## Funding

This work was financed by the NSFC National Natural Science Foundation of China (11972280).

## Conflict of interest

The authors declare no conflicts of interest.

## Author contributions

*Conceptualization:* Yanshen Yang, Feng Xu

*Investigation:* Yanshen Yang, Yuanbo Jia

*Writing – original draft:* Yanshen Yang

*Writing – review & editing:* Feng Xu, Qingzhen Yang

## Ethics approval and consent to participate

Not applicable.

## Consent for publication

Not applicable.

## Availability of data

Not applicable.

## References

1. Song H-HG, Rumma RT, Ozaki CK, *et al.*, 2018, Vascular tissue engineering: Progress, challenges, and clinical promise. *Cell Stem Cell*, 22(3): 340–354.
2. Khademhosseini A, Langer R, 2016, A decade of progress in tissue engineering. *Nat Protoc*, 11(10): 1775–1781.
3. Zhang P, Zhang C, Li J, *et al.*, 2019, The physical microenvironment of hematopoietic stem cells and its emerging roles in engineering applications. *Stem Cell Res Ther*, 10(1): 327.
4. Xing F, Li L, Zhou C, *et al.*, 2019, Regulation and directing stem cell fate by tissue engineering functional microenvironments: Scaffold physical and chemical cues. *Stem Cells Int*, 2019: 2180925.
5. Agrawal A, Suryakumar G, Rathor R, 2018, Role of defective Ca<sup>2+</sup> signaling in skeletal muscle weakness: Pharmacological implications, *J Cell Commun Signal*, 12(4): 645–659.
6. Vandenburg HH, 1987, Motion into mass: How does tension stimulate muscle growth? *Med Sci Sports Exerc*, 19(5): S142–9.
7. Emon B, Bauer J, Jain Yasna, *et al.*, 2018, Biophysics of tumor microenvironment and cancer metastasis—A mini review. *Comput Struct Biotechnol J*, 16: 279–287.
8. Mierke CT, 2019, The matrix environmental and cell mechanical properties regulate cell migration and contribute to the invasive phenotype of cancer cells. *Rep Prog Phys*, 82(6): 64602.
9. Engler AJ, Sen S, Sweeney HL, *et al.*, 2006, Matrix elasticity directs stem cell lineage specification. *Cell*, 126(4): 677–689.
10. Qiu Y, Ciciliano J, Myers DR, *et al.*, 2015, Platelets and physics: How platelets “feel” and respond to their mechanical microenvironment. *Blood Rev*, 29(6): 377–386.
11. Fontoura JC, Viezzer C, Santos FGDS, *et al.*, 2020, Comparison of 2D and 3D cell culture models for cell growth, gene expression and drug resistance. *Mater Sci Eng C Mater Sci Eng App*, 107: 110264.
12. Derakhshanfar S, Mbeleck R, Xu K, *et al.*, 2018, 3D bioprinting for biomedical devices and tissue engineering: A review of recent trends and advances. *Bioact Mater*, 3(2): 144–156.
13. Yang H, Yang K-H, Narayan RJ, *et al.*, 2021, Laser-based bioprinting for multilayer cell patterning in tissue engineering and cancer research. *Essays Biochem*, 65(3): 409–416.
14. Ouyang L, 2022, Pushing the rheological and mechanical boundaries of extrusion-based 3D bioprinting. *Trends Biotechnol*, 40(7): 891–902.
15. Felipe-Mendes C, Ruiz-Rubio L, Vilas-Vilela JL, 2020, Biomaterials obtained by photopolymerization: From UV to two photon. *Emerg Mater*, 3(4): 453–468.
16. Dey M, Ozbolat IT, 2020, 3D bioprinting of cells, tissues and organs, *Sci Rep*. 10(1): 14023.
17. Janmey PA, 1998, The cytoskeleton and cell signaling: Component localization and mechanical coupling. *Physiol Rev*, 78(3): 763–781.
18. Fletcher DA, Mullins RD, 2010, Cell mechanics and the cytoskeleton. *Nature*, 463(7280): 485–492.
19. Fishkind DJ, Wang Y-I, 1995, New horizons for cytokinesis. *Curr Opin Cell Biol*, 7(1): 23–31.
20. Stossel TP, 1994, The machinery of cell crawling. *Sci Am*, 271(3): 54–55, 58–63.
21. Damania D, Subramanian H, Tiwari AK, *et al.*, 2010, Role of cytoskeleton in controlling the disorder strength of cellular nanoscale architecture, *Biophys J*, 99(3): 989–996.
22. Janmey P, 1995, *Structure and Dynamics of Membranes*, Elsevier Sci, North Holland, 114–717.
23. Dupont S, Morsut L, Aragona M, *et al.*, 2011, Role of YAP/TAZ in mechanotransduction. *Nature*, 474(7350): 179–183.
24. Owens DJ, Messéant J, Moog S, *et al.*, 2020, Lamin-related congenital muscular dystrophy alters mechanical signaling and skeletal muscle growth. *Int J Mol Sci*, 22(1): 306.
25. Parreno J, Raju S, Wu P-H, *et al.*, 2017, MRTF-A signaling regulates the acquisition of the contractile phenotype in dedifferentiated chondrocytes. *Mat Bio J Intl Soc Mat Bio*, 62: 3–14.
26. Kim N-G, Koh E, Chen X, *et al.*, 2011, E-cadherin mediates contact inhibition of proliferation through hippo signaling-pathway components. *Proc Natl Acad Sci USA*, 108(29): 11930–11935.
27. Rando TA, 2001, The dystrophin-glycoprotein complex, cellular signaling, and the regulation of cell survival in the muscular dystrophies. *Muscl Nerve*, 24(12): 1575–1594.
28. Guimarães CF, Gasperini L, Marques AP, *et al.*, 2020, The stiffness of living tissues and its implications for tissue engineering. *Nat Rev Mater*, 5(5): 351–370.
29. Rho JY, Ashman RB, Turner CH, 1993, Young’s modulus of trabecular and cortical bone material: Ultrasonic and microtensile measurements. *J Biomech*, 26(2): 111–119.
30. Sotres J, Jankovskaja S, Wannerberger K, *et al.*, 2017, Ex-vivo force spectroscopy of intestinal mucosa reveals the mechanical properties of mucus blankets. *Sci Rep*, 7(1): 7270.
31. Masuzaki R, Tateishi R, Yoshida H, *et al.*, 2007, Assessing liver tumor stiffness by transient elastography. *Hepatol Int*, 1(3): 394–397.
32. Darling EM, Topel M, Zauscher S, *et al.*, 2008, Viscoelastic properties of human mesenchymally-derived stem cells and primary osteoblasts, chondrocytes, and adipocytes. *J Biomech*, 41(2): 454–464.

33. Banaszkiwicz PA, Kader DE, 2014, The compressive behavior of bone as a two-phase porous structure, in *Classic Papers in Orthopaedics*, Springer, London, 457–460.
34. Hayashi K, Iwata M, 2015, Stiffness of cancer cells measured with an AFM indentation method. *J Mech Behav Biomed Mater*, 49: 105–111.
35. Yousafzai MS, Coceano G, Bonin S, *et al.*, 2017, Investigating the effect of cell substrate on cancer cell stiffness by optical tweezers. *J Biomech*, 60: 266–269.
36. Milovanovic P, Potocnik J, Djonic D, *et al.*, 2012, Age-related deterioration in trabecular bone mechanical properties at material level: Nanoindentation study of the femoral neck in women by using AFM. *Exp Gerontol*, 47(2): 154–159.
37. Gentili C, Cancedda R, 2009, Cartilage and bone extracellular matrix. *Curr Pharm Design*, 15(12): 1334–1348.
38. Najafi M, Farhood B, Mortezaee K, 2019, Extracellular matrix (ECM) stiffness and degradation as cancer drivers. *J Cell Biochem*, 120(3): 2782–2790.
39. Berdyeva TK, Woodworth CD, Sokolov I, 2005, Human epithelial cells increase their rigidity with ageing in vitro: Direct measurements. *Phys Med Biol*, 50(1): 81–92.
40. Kato S, Espinoza N, Lange S, *et al.*, 2008, Characterization and phenotypic variation with passage number of cultured human endometrial adenocarcinoma cells. *Tissue Cell*, 40(2): 95–102.
41. Kiricuta IC, Simplăceanu V, 1975, Tissue water content and nuclear magnetic resonance in normal and tumor tissues. *Cancer Res*, 35(5): 1164–1167.
42. Dhume RY, Barocas VH, 2019, Emergent structure-dependent relaxation spectra in viscoelastic fiber networks in extension. *Acta Biomater*, 87: 245–255.
43. Chaudhuri O, Gu L, Klumpers D, *et al.*, 2016, Hydrogels with tunable stress relaxation regulate stem cell fate and activity. *Nat Mater*, 15(3): 326–334.
44. Chaudhuri O, Gu L, Darnell M, *et al.*, 2015, Substrate stress relaxation regulates cell spreading. *Nat Comm*, 6: 6364.
45. Adebowale K, Gong Z, Hou JC, *et al.*, 2021, Enhanced substrate stress relaxation promotes filopodia-mediated cell migration. *Nat Mater*, 20(9): 1290–1299.
46. Magdalena D, Michał W, Christopher BA, 2019, The effect of a stylus tip on roundness deviation with different roughness. *Adv Manuf II*, 147–157.
47. Smith JR, Breakspear S, Campbell SA, 2003, AFM in surface finishing: Part II. Surface roughness. *Trans IMF*, 81(3): B55–B58.
48. Yilbas Z, Hasmi MSJ, 1999, Surface roughness measurement using an optical system, *J Mater Process Technol*, 88(1-3): 10–22.
49. Hameed NA, Ali IM, Hassun HK, 2019, Calculating surface roughness for a large scale SEM images by mean of image processing. *Energy Procedia*, 157: 84–89.
50. Anselme K, Bigerelle M, 2011, Role of materials surface topography on mammalian cell response. *Int Mater Rev*, 56(4): 243–266.
51. Hersel U, Dahmen C, Kessler H, 2003, RGD modified polymers: Biomaterials for stimulated cell adhesion and beyond. *Biomaterials*, 24(24): 4385–4415.
52. Carvalho JL, Miranda de Goes A, Gomes DA, *et al.*, 2013, *Innovative Strategies for Tissue Engineering*, INTECH Open Access Publisher. London, United Kingdom, 295–313.
53. Kim D-H, Lipke EA, Kim P, *et al.* 2010, Nanoscale cues regulate the structure and function of macroscopic cardiac tissue constructs. *Proc Natl Acad Sci USA*, 107(2): 565–570.
54. Fujita S, Ohshima M, Iwata H, 2009, Time-lapse observation of cell alignment on nanogrooved patterns. *J R Soc Interface*, 6 Suppl(3): S269–77.
55. Tatsumi R, Sheehan SM, Iwasaki H, *et al.*, 2001, Mechanical stretch induces activation of skeletal muscle satellite cells in vitro. *Exp Cell Res*, 267(1): 107–114.
56. Albro MB, Nims RJ, Cigan AD, *et al.*, 2013, Accumulation of exogenous activated TGF- $\beta$  in the superficial zone of articular cartilage. *Biophys J*, 104(8): 1794–1804.
57. Wong VW, Levi K, Akaishi S, *et al.*, 2012, Scar zones: Region-specific differences in skin tension may determine incisional scar formation. *Plast Reconstr Surg*, 129(6): 1272–1276.
58. Storm C, Pastore JJ, MacKintosh FC, *et al.*, 2005, Nonlinear elasticity in biological gels. *Nature*, 435(7039): 191–194.
59. Heyes CD, Groll J, Möller M, *et al.*, 2007, Synthesis, patterning and applications of star-shaped poly(ethylene glycol) biofunctionalized surfaces. *Mol Biosyst*, 3(6): 419–430.
60. Al-Nimry S, Dayah AA, Hasan I, *et al.*, 2021, Cosmetic, biomedical and pharmaceutical applications of fish gelatin/hydrolysates. *Marine Drugs*, 19(3): 145.
61. Franchi M, Trirè A, Quaranta M, *et al.*, 2007, Collagen structure of tendon relates to function. *Sci World J*, 7: 404–420.
62. Soofi SS, Last JA, Liliensiek SJ, *et al.*, 2009, The elastic modulus of matrigel as determined by atomic force microscopy. *J Struct Biol*, 167(3): 216–219.
63. Bassani F, 2005, *Encyclopedia of Condensed Matter Physics*, Elsevier. Cambridge, Massachusetts, United States, 103–105.
64. Salam Hamdy MA, Abu-Thabit NY, 2018, Stimuli-responsive biopolymer nanocarriers for drug delivery applications. *Types Triggers*, 1: 405–432.
65. Tilak D, Yimin Q, 2016, *Medical Textile Materials*, Woodhead Publishing. Sawston, Cambridge, United Kingdom, 31–33.
66. Vieira AC, Vieira JC, Guedes RM, *et al.*, 2010, Degradation and viscoelastic properties of PLA-PCL, PGA-PCL, PDO and PGA Fibres. *Mater Sci Forum*, 636–637: 825–832.
67. Hodgkinson R, Currey JD, Evans GP, 1989, Hardness, an indicator of the mechanical competence of cancellous bone. *J Orthop Res*, 7(5): 754–758.

68. Wu Y, Xiang Y, Fang J, *et al.*, 2019, The influence of the stiffness of GelMA substrate on the outgrowth of PC12 cells. *Biosci Rep*, 39(1): BSR20181748.
69. Elkhoury K, Morsink M, Tahri Y, *et al.*, 2021, Synthesis and characterization of C2C12-laden gelatin methacryloyl (GelMA) from marine and mammalian sources. *Int J Biol Macromol*, 183: 918–926.
70. Duan B, Kapetanovic E, Hockaday LA, *et al.*, 2014, Three-dimensional printed trileaflet valve conduits using biological hydrogels and human valve interstitial cells. *Acta Biomater*, 10(5): 1836–1846.
71. Subramani R, Izquierdo-Alvarez A, Bhattacharya P, *et al.*, 2020, The influence of swelling on elastic properties of polyacrylamide hydrogels. *Front Mater*, 7: 212.
72. Li Z, Liu Z, Ng TY, *et al.*, 2020, The effect of water content on the elastic modulus and fracture energy of hydrogel. *Extreme Mech Lett*, 35: 100617.
73. Wu F, Pang Y, Liu J, 2020, Swelling-strengthening hydrogels by embedding with deformable nanobarriers. *Nat Commun*, 11(1): 4502.
74. Islam MR, Virag J, Oyen ML, 2020, Micromechanical poroelastic and viscoelastic properties of ex-vivo soft tissues. *J Biomech*, 113: 110090.
75. Kuzucu M, Vera G, Beaumont M, *et al.*, 2021, Extrusion-based 3D bioprinting of gradients of stiffness, cell density, and immobilized peptide using thermogelling hydrogels. *ACS Biomater Sci Eng*, 7(6): 2192–2197.
76. Wang M, Li W, Mille LS, *et al.*, 2022, Digital light processing based bioprinting with composable gradients. *Adv Mater*, 34(1): e2107038.
77. Prendergast ME, Davidson MD, Burdick JA, 2021, A biofabrication method to align cells within bioprinted photocrosslinkable and cell-degradable hydrogel constructs via embedded fibers. *Biofabrication*, 13(4): 044108.
78. Swartz MA, Tschumperlin DJ, Kamm RD, *et al.*, 2001, Mechanical stress is communicated between different cell types to elicit matrix remodeling. *Proc Natl Acad Sci USA*, 98(11): 6180–6185.
79. Li X, Tsutsui Y, Matsunaga T, *et al.*, 2011, Precise control and prediction of hydrogel degradation behavior. *Macromolecules*, 44(9): 3567–3571.
80. Lou J, Stowers R, Nam S, *et al.*, 2018, Stress relaxing hyaluronic acid-collagen hydrogels promote cell spreading, fiber remodeling, and focal adhesion formation in 3D cell culture. *Biomaterials*, 154: 213–222.
81. Nam S, Stowers R, Lou J, *et al.*, 2019, Varying PEG density to control stress relaxation in alginate-PEG hydrogels for 3D cell culture studies. *Biomaterials*, 200: 15–24.
82. Yang Q, Gao B, Xu F, 2020, Recent advances in 4D bioprinting. *Biotechnol J*, 15(1): e1900086.
83. Jing Y, Yang B, Yuan W, *et al.*, 2021, Dynamic cell-adaptable hydrogels with a moderate level of elasticity promote 3D development of encapsulated cells. *Appl Mater Today*, 22: 100892.
84. Arani A, Arunachalam SP, Chang IC, *et al.*, 2017, Cardiac MR elastography for quantitative assessment of elevated myocardial stiffness in cardiac amyloidosis. *J Magn Reson Imaging*, 46(5): 1361–1367.
85. Domian IJ, Yu H, Mittal N, 2017, On materials for cardiac tissue engineering. *Adv Healthc Mater*, 6(2): 1600768.
86. Marinelli JP, Levin DL, Vassallo R, *et al.*, 2017, Quantitative assessment of lung stiffness in patients with interstitial lung disease using MR elastography. *Adv Healthc Mater*, 46(2): 365–374.
87. Mariappan YK, Glaser KJ, Levin DL, *et al.*, 2014, Estimation of the absolute shear stiffness of human lung parenchyma using (1) H spin echo, echo planar MR elastography. *J Magn Reson Imaging*, 40(5): 1230–1237.
88. Booth AJ, Hadley R, Cornett AM, *et al.*, 2012, Acellular normal and fibrotic human lung matrices as a culture system for in vitro investigation. *Am J Respir Crit Care*, 186(9): 866–876.
89. Cha SW, Jeong WK, Kim Y, *et al.*, 2014, Nondiseased liver stiffness measured by shear wave elastography: A pilot study. *J Med Ultrasound*, 33(1): 53–60.
90. Ling W, Lu Q, Lu C, *et al.*, 2014, Effects of vascularity and differentiation of hepatocellular carcinoma on tumor and liver stiffness: In vivo and in vitro studies. *Ultrasound Med Biol*, 40(4): 739–746.
91. Yeh W-C, Li P-C, Jeng Y-M, *et al.*, 2002, Elastic modulus measurements of human liver and correlation with pathology. *Ultrasound Med Biol*, 28(4): 467–474.
92. Lee DH, Lee JM, Han JK, *et al.*, 2013, MR elastography of healthy liver parenchyma: Normal value and reliability of the liver stiffness value measurement. *J Magn Reson Imaging*, 38(5): 1215–1223.
93. Venkatesh SK, Wang G, Teo LL, *et al.*, 2014, Magnetic resonance elastography of liver in healthy Asians: Normal liver stiffness quantification and reproducibility assessment. *J Magn Reson Imaging*, 39(1): 1–8.
94. Johnson B, Campbell S, Campbell-Kyureghyan N, 2021, Characterizing the material properties of the kidney and liver in unconfined compression and probing protocols with special reference to varying strain rate. *Biomechanics*, 1(2): 264–280.
95. Pozzi R, Parzanese I, Baccarin A, *et al.*, 2017, Point shear-wave elastography in chronic pancreatitis: A promising tool for staging disease severity. *Pancreatology*, 17(6): 905–910.
96. An H, Shi Y, Guo Q, *et al.*, 2016, Test-retest reliability of 3D EPI MR elastography of the pancreas. *Clin Radiol*, 71(10): 1068.e7–1068.e12.
97. Gou M, Zheng M, Zhao Y, *et al.*, 2017, Mechanical property of PEG hydrogel and the 3D red blood cell microstructures

- fabricated by two-photon polymerization. *Appl Surf Sci*, 416: 273–280.
98. DeKosky BJ, Dormer NH, Ingavle GC, *et al.*, 2010, Hierarchically designed agarose and poly(ethylene glycol) interpenetrating network hydrogels for cartilage tissue engineering. *Tissue Eng Part C Methods*, 16(6): 1533–1542.
99. Lanasa SM, Hoffecker IT, Bryant SJ, 2011, Presence of pores and hydrogel composition influence tensile properties of scaffolds fabricated from well-defined sphere templates. *J Biomed Mater Res Part B Appl Bio Mater*, 96(2): 294–302.
100. Gunn JW, Turner SD, Mann BK, 2005, Adhesive and mechanical properties of hydrogels influence neurite extension. *J Biomed Mater Res Part A*, 72(1): 91–97.
101. Alam K, Umer J, Iqbal M, *et al.*, 2020, Measurements of elastic properties of biological hydrogels using atomic force microscopy. *J Phys Conf Series*, 1455(1): 12012.
102. Yin J, Yan M, Wang Y, *et al.*, 2018, 3D bioprinting of low-concentration cell-laden gelatin methacrylate (GelMA) bioinks with a two-step cross-linking strategy. *ACS Appl Mater Interfaces*, 10(8): 6849–6857.
103. West ER, Xu M, Woodruff TK, *et al.*, 2007, Physical properties of alginate hydrogels and their effects on in vitro follicle development. *Biomaterials*, 28(30): 4439–4448.
104. Alcaraz J, Mori H, Ghajar CM, *et al.*, 2011, Collective epithelial cell invasion overcomes mechanical barriers of collagenous extracellular matrix by a narrow tube-like geometry and MMP14-dependent local softening. *Integr Biol*, 3(12): 1153–1166.